

# Surface and Interfacial Waves over Currents and Point-Vortices

Chris Curtis

Department of Mathematics and Statistics  
San Diego State University

November 3, 2016

# Collaborators

- Henrik Kalisch (U. of Bergen)
- Katie Oliveras (Seattle U.)
- Theresa Morrison (SDSU)

# Waves over Depth-Varying Currents and Vortices

- Currents are ubiquitous in fluids. How do they interact with free surfaces and interfaces?
- Eddies are ubiquitous as well. Same question.
- How much of the above questions can we answer with simple vorticity models?

# Depth-Varying Currents

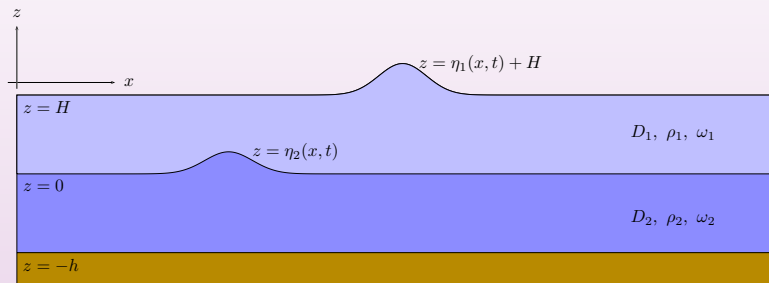


Figure: Density stratified fluid with piecewise constant vorticity.

# Depth Varying Currents

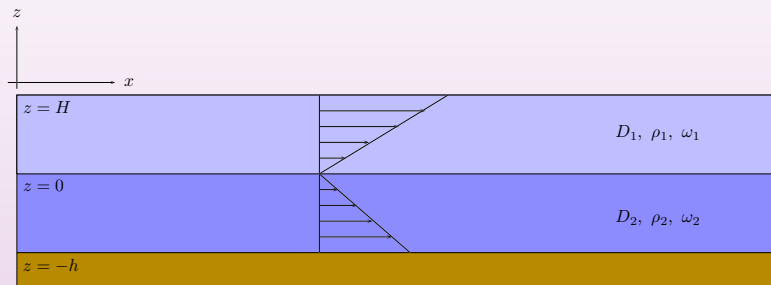
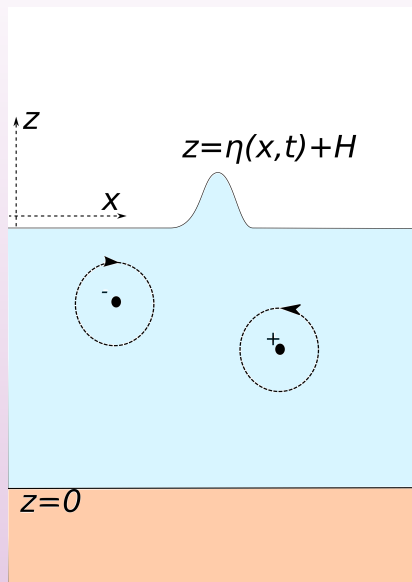


Figure: Discontinuous Linear Shear Profiles.

# Irrotational Point Vortices



# The DNO and AFM Methods

- To close our system in terms of surface height  $\eta$  and surface velocity potential  $q$ , we introduce the DNO  $G(\eta)$  (see the work of Craig and collaborators) so that

$$\eta_t = G(\eta)q.$$

- A complimentary point of view to doing this is the method of Ablowitz, Fokas, and Mussilimani (AFM). One can readily show the AFM and DNO approaches are formally equivalent.
- AFM leverages solving  $\Delta\phi = 0$  so that you can turn the boundary equation into the equivalent set of integral equations

$$\int e^{-ikx} (\cosh(k(\eta + h))\eta_t + iq_x \sinh(k(\eta + h))) dx = 0, \quad k \neq 0.$$

# Outline

- **Part I:** We use the AFM approach to deal with the depth-varying currents, derive shallow-water approximations, and present numerical results of dynamics.
- **Part II:** We use a modified version of AFM to rewrite the problem in terms of surface variables and vortex positions alone. We then use the DNO to build numerical schemes.

# Part I: Waves over Currents

- The constant vorticity and shear flow literature is far too vast to summarize.
- Civil engineer, Dalrymple, began looking at layer models to study more general density and shear profiles.
- Maslow and Redekopp also study arbitrary incompressible density/shear profiles varying in vertical.
- Generally, one surface, or rigid lid/internal layer is studied.

# Problem Formulation

- Restricting ourselves to a linear shear, or constant vorticity, background flow within each layer of the fluid ( $j = 1, 2$ ), Euler's equations of motion for  $(x, z) \in D_j$  become

$$\nabla \cdot \mathbf{u}_j = 0, \quad (1)$$

$$\nabla \times \mathbf{u}_j = \omega_j \hat{\mathbf{y}} \quad (2)$$

$$\partial_t \mathbf{u}_j + \mathbf{u}_j \cdot \nabla \mathbf{u}_j = -\frac{1}{\rho_j} \nabla p_j - g \hat{\mathbf{z}}, \quad (3)$$

where  $\mathbf{u}_j = [u_j \ v_j]^T$  represents the fluid velocities in  $D_j$ .

# Problem Formulation

- At the various interfaces, we enforce the kinematic boundary conditions

$$v_2 = 0, \quad z = -h, \quad (4)$$

$$\partial_t \eta_1 = v_1 - u_1 \partial_x \eta_1, \quad z = \eta_1(x, t) + H, \quad (5)$$

$$\partial_t \eta_2 = v_1 - u_1 \partial_x \eta_2, \quad z = \eta_2^+(x, t) \quad (6)$$

$$\partial_t \eta_2 = v_2 - u_2 \partial_x \eta_2, \quad z = \eta_2^-(x, t) \quad (7)$$

as well as the pressure relations given by

$$p_1 = p_c, \quad z = \eta_1(x, t) + H, \quad (8)$$

$$p_1 = p_2, \quad z = \eta_2(x, t). \quad (9)$$

By  $\eta_2^+$  and  $\eta_2^-$  we mean the regions just above and just below the surface  $z = \eta_2(x, t)$  respectively.

# Problem Formulation

- Using  $\mathbf{u}_j = \omega_j z \hat{\mathbf{z}} + \nabla \phi$  coupled with AFM, we can find a closed system describing the evolution of the surface and internal layer.
- We rescale the bistratified, bilinear shear system via the following non-dimensional parameters

$$\tilde{x} = x/L, \quad \tilde{z} = z/H, \quad \tilde{t} = \frac{\sqrt{gH}}{L} t, \quad \tilde{k} = Lk,$$

$$\eta_j = a\tilde{\eta}_j, \quad Q = \frac{agL}{\sqrt{gH}} \tilde{Q}, \quad q_j = \frac{agL}{\sqrt{gH}} \tilde{q}_j.$$

- Take the balances

$$\frac{H}{h} = \frac{1}{\tilde{d}}, \quad \frac{a}{H} = \epsilon, \quad \frac{H}{L} = \gamma, \quad \omega_j \sqrt{\frac{H}{g}} = \tilde{\omega}_j, \quad \frac{\rho_2}{\rho_1} = \tilde{\rho},$$

# Problem Formulation

- While complicated, AFM formulation readily allows for asymptotically reduced models to be derived.
- However, just putting interfaces next to one another is not always physically sensible i.e. what about Kelvin–Helmholtz instabilities?

# Kelvin–Helmholtz Instabilities

- Using  $e^{-ikx+i\Omega t}$ , we find the dispersion relationship

$$\begin{aligned}\Pi = & k^4 \left( (\rho + \bar{d}s^2 \varphi(s) \varphi(\bar{d}s)) \tilde{\Omega}^4 + (\rho(\omega_1 \varphi(s) + \omega_2 \bar{d} \varphi(\bar{d}s)) - 2\rho\omega_1 \right. \\ & + (\rho\omega_1^2 - \rho(1 + \omega_1^2))\varphi(s) + (\omega_1^2 - 2\omega_1\omega_2\rho - \rho)\bar{d}\varphi(\bar{d}s) + \omega_1(\omega_1 \\ & + \bar{d}\varphi(\bar{d}s) (2\omega_1(\rho - 1) + \omega_1^2(\omega_2\rho - \omega_1) + (2\omega_1 - \rho(\omega_1 + \omega_2 + \\ & \left. + (\rho - 1)\bar{d}\varphi(\bar{d}s)(-\omega_1^2 + \varphi(s)(1 + \omega_1^2))) \right)\end{aligned}$$

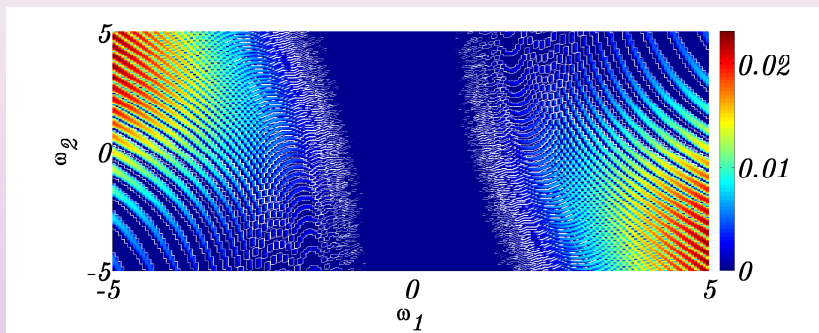
where  $s = \gamma k$ ,  $\tilde{\Omega} = \Omega/k$ , and

$$\varphi(s) = \frac{\tanh(s)}{s}.$$

- I know I left a formula trailing off the edge of the slide. But that kind of makes my point.

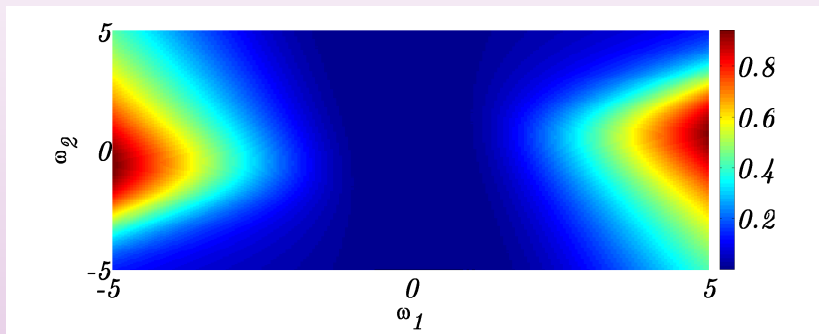
# Kelvin–Helmholtz Instabilities

- Taking  $\bar{d} \ll 1$ , we can use asymptotic arguments to show there are shear/density configurations for which only real spectra can be found for all wave numbers.
- Letting  $\bar{d} = .25$ ,  $\rho = 820$ , we get the following plot of the maximum imaginary part of the spectrum for  $0 \leq s \leq 300$ .



# Kelvin–Helmholtz Instabilities

- Letting  $\bar{d} = 4$ ,  $\rho = 1.5$ , we get the following plot of the maximum imaginary part of the spectrum for  $0 \leq s \leq 300$ .



# Reduced Model/System of KdV equations

- To capture nonlinear effects, we take the balance  $\epsilon = \gamma^2$ , and then expand in  $\epsilon$ .
- From  $\epsilon = 0$  problem, we have four wave speeds  $\lambda_j$  as  $\epsilon \rightarrow 0$ .

- This ultimately leads to four KdV equations of the form

$$c_{nl}(\lambda_j)w_j^{(0)}\partial_{\xi_j}w_j^{(0)} + c_d(\lambda_j)\partial_{\xi_j}^3w_j^{(0)} + c_t(\lambda_j)\partial_{\tau}w_j^{(0)} = 0,$$

- This allows us to recreate the surface profiles via the equations

$$\eta_1(x, t) \sim \sum_{j=1}^4 (1 - \rho + \rho(\bar{d}\omega_2\lambda_j + \lambda_j^2)/\bar{d})w_j^{(0)}(x - \lambda_j t, \epsilon t),$$

$$\eta_2(x, t) \sim \sum_{j=1}^4 w_j^{(0)}(x - \lambda_j t, \epsilon t).$$

# Finding Nonlinear Response: Strong Stratification

- Define

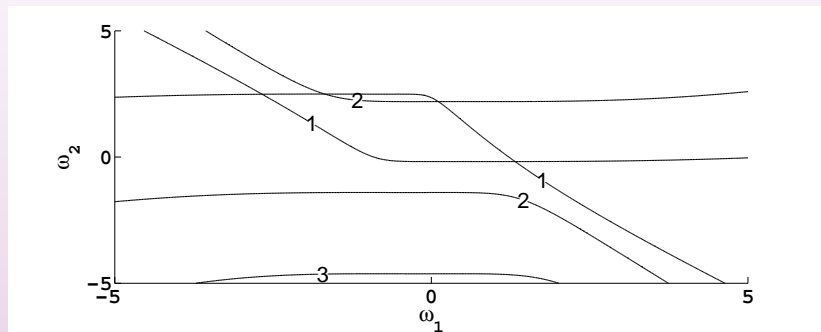
$$c_b(\lambda) = \frac{c_{nl}(\lambda)}{6c_d(\lambda)c_t(\lambda)} \left( \lambda + (\lambda^2 - \omega_1\lambda - 1) \left( \frac{1-\rho}{\lambda} + \rho \right) + 1 \right),$$

- Looking at  $c_b(\lambda_j)$ , we can determine when we expect large initial conditions in the rescaled KdV equation

$$\tilde{w}_\tau + \partial_\xi^3 \tilde{w} + \tilde{w} \partial_\xi \tilde{w} = 0.$$

- Roughly, the larger the initial condition that goes into this rescaled equation, the more nonlinear phenomena we expect to see.

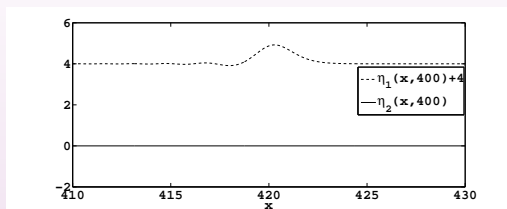
# Finding Nonlinear Response: Strong Stratification



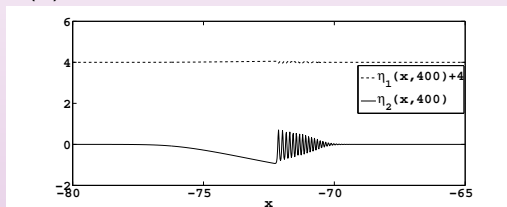
$\log_{10}(|c_b(\lambda_2)|), \log_{10}(|c_b(\lambda_3)|)$

Figure: Contour plots of  $c_b(\lambda_j)$  for  $\rho = 820$  and  $\bar{d} = .25$ .

# Finding Nonlinear Response: Strong Stratification



(a) Surface wave for  $410 \leq x \leq 430$ .



(b) Internal wave for  $-80 \leq x \leq -65$ .

Figure:  $\omega_1 = .1$ ,  $\omega_2 = -4.62$ ,  $\rho = 820$ ,  $\bar{d} = .25$ , and  $\epsilon = .0025$ .

# Conclusion for Part One

- Shear and density variation can result in significant nonlinear wave response, especially along internal layers.
- Hints at a wide variety of phenomena in the presence of more layers.
- Also calls for higher order, or fully nonlinear solves.
- Traveling waves? Almost done with K. Oliveras... fully nonlinear, and stability.

## Part II: Point Vortices under Waves

- In 2D, for vorticity  $\omega(\mathbf{x}, t)$  we have

$$\omega_t + \mathbf{u} \cdot \nabla \omega = 0.$$

- Close the system via Biot-Savart and harmonic potential  $\phi$  so that

$$\mathbf{u} = \int \mathbf{K}(\mathbf{x} - \mathbf{y}) \omega(\mathbf{y}, t) d\mathbf{y} + \nabla \phi.$$

- Let

$$\omega(\mathbf{x}, t) = \frac{1}{2\pi} \sum_{j=1}^N \Gamma_j \delta(\mathbf{x} - \mathbf{x}_j(t)),$$

and so we can approximate arbitrary vorticity profiles (technical details: see Cottet et al., Krasny, and several others) via irrotational point vortices.

# Irrotational Vortices under Waves

- The fluid velocity  $\mathbf{u}$  is given by the gradient of a potential, say  $\phi$  where

$$\phi(x, z, t) = \phi_v(x, z, t) + \tilde{\phi}(x, z, t).$$

- $\phi_v$  is defined to be

$$\phi_v(x, z, t) = \frac{1}{2\pi} \sum_{j=1}^N \Gamma_j \phi_{v,j}(x, z, t),$$

with  $\Gamma_j$  denoting the circulation strength of the vortices and

$$\phi_{v,j}(x, z, t) = \Phi_\rho(x - x_j(t), z - z_j(t)) - \Phi_\rho(x - x_j(t), z + z_j(t)),$$

where

$$\Phi_\rho(x, z) = \sum_{m=-\infty}^{\infty} \tan^{-1} \left( \frac{z}{x - 2mL} \right).$$

# Irrotational Vortices under Waves

- This modifies the boundary equations so that

$$\eta_t = -\eta_x \tilde{\phi}_x + \tilde{\phi}_z + P_v(x_1, z_1, \dots, x_N, z_N),$$

and

$$\tilde{\phi}_t + \frac{1}{2} |\nabla \tilde{\phi}|^2 + g\eta = -\nabla \phi_v \cdot \nabla \phi + E_v(x_1, z_1, \dots, x_N, z_N)$$

- Apologies, but  $P_v$  and  $E_v$  are not very nice to look at.

# Irrotational Vortices under Waves

- Likewise we now tack on the ODE's

$$\dot{x}_j = \frac{1}{4L} \left( \Gamma_j \operatorname{cotanh} \left( \frac{\pi z_j}{L} \right) + 2 \sum_{l \neq j} \Gamma_l v_{jl}^{(h)} \right) + \tilde{\phi}_x(x_j, z_j, t),$$

$$\dot{z}_j = \frac{1}{2L} \sinh \left( \frac{\pi}{L} z_j \right) \sum_{l \neq j} \Gamma_l v_{jl}^{(v)} + \tilde{\phi}_z(x_j, z_j, t),$$

- $v_{jl}^{(h)}$  and  $v_{jl}^{(v)}$  are even worse to look at.

# Irrotational Vortices under Waves

- So AFM lets us write for  $\tilde{\eta}_t = \eta_t - P_v$

$$\int_{-L}^L e^{-i\pi kx/L} (\cosh(k(\eta + H))\tilde{\eta}_t + i\tilde{q}_x \sinh(k(\eta + H))) dx = 0$$

- But now we need  $\tilde{\phi}_x(x_j, z_j, t)$  and  $\tilde{\phi}_z(x_j, z_j, t)$  in terms of surface variables and vortex positions alone to close the system.
- Modify original AFM argument by introducing fundamental solutions

$$\psi_j(x, z, t) = -\frac{1}{4\pi} \sum_{m=-\infty}^{\infty} \left( \ln \left( \tilde{x}_{j,m}^2 + \tilde{z}_{j,-}^2 \right) + \ln \left( \tilde{x}_{j,m}^2 + \tilde{z}_{j,+}^2 \right) \right)$$

# Irrotational Vortices under Waves

- Use Green's third identity and some tricks, we end up with

$$\tilde{\phi}_x(x_j, z_j, t) = - \int_{-L}^L ((\eta_t - P_v) \partial_x \psi_j + \tilde{q}_x \partial_z \psi_j) \Big|_{z=\eta+H} dx$$

- Likewise we can show

$$\tilde{\phi}_z(x_j, z_j, t) = - \int_{-L}^L ((\eta_t - P_v) \partial_z \tilde{\psi}_j - \tilde{q}_x \partial_x \tilde{\psi}_j) \Big|_{z=\eta+H} dx$$

- So we have now closed the system in terms of surface variables and vortex positions alone.

# Shallow-Water Scalings

- We now choose the following non-dimensionalizations

$$\tilde{x} = \frac{x}{L}, \quad \tilde{z} = \frac{z}{H}, \quad \tilde{t} = \frac{\sqrt{gH}}{L} t, \quad \eta = d\tilde{\eta}, \quad \tilde{\phi} = \mu L \sqrt{gH} \tilde{\phi},$$

where we define the non-dimensional parameters

$$\mu = \frac{d}{H}, \quad \gamma = \frac{H}{L},$$

and where we define the Froude number  $F$  to be

$$F = \frac{\Gamma}{\mu L \sqrt{gH}}.$$

# Shallow-Water Scalings

- From now on, the Froude number determines the strength of vortex interactions.
- Can now readily find the DNO expansion

$$\eta_t - \frac{1}{\gamma} P_v(x, 1 + \mu\eta, t) = \left( G_0 + \mu G_1 + \mu^2 G_2 + \dots \right) Q$$

where  $Q = \tilde{q}_x$ .

- Numerically simple and fast to implement. Extends to 3D.
- But David Ambrose has a point.

# Numerics

- Pseudo-spectral in space, 4th order Runge-Kutta in time.
- If we run to time  $t_f$ , truncate DNO expansion when

$$\frac{\|G_{\tilde{N}}Q\|_2}{\|Q\|_2} \leq \text{mach. prec.}$$

- The range here is  $18 \leq \tilde{N} \leq 35$ .
- Orszag's 2/3-rule is used for filtering.
- Quiescent fluid: we track energy input into the surface via

$$E(t) = \frac{1}{2} \int_{-1}^1 qG(\eta)Qdx + \frac{1}{2} \int_{-1}^1 \eta^2 dx.$$

# Numerics: Cnoidal Waves

- Can show as  $F \rightarrow 0$ , we can derive KdV equation

$$2Q_\tau + 3QQ_\xi + \frac{1}{3}Q_{\xi\xi\xi} = 0$$

- Thus we can look at how vortices modify propagation of 'cnoidal' profiles where

$$Q(x, t) \sim \frac{2}{3}q_0 + \frac{4}{3}\tilde{m}^2\mathcal{K}^2(\tilde{m})\text{cn}^2(\mathcal{K}(\tilde{m})(x - (1 + \mu\tilde{c})t); \tilde{m})$$

$$\eta(x, t) \sim \left(1 + \frac{2}{3}\mu\mathcal{K}^2(\tilde{m})(2\tilde{m}^2 - 1)\right) Q(x, t)$$

$$\tilde{c} = \frac{2}{3}\mathcal{K}^2(\tilde{m})(2\tilde{m}^2 - 1) + q_0$$

# Numerics: Cnoidal Waves

- Place two vortices of opposite signs at

$$x_1(0) = -\mu\gamma, \quad x_2(0) = \mu\gamma, \quad z_1(0) = z_2(0) = .25.$$

- Then we get

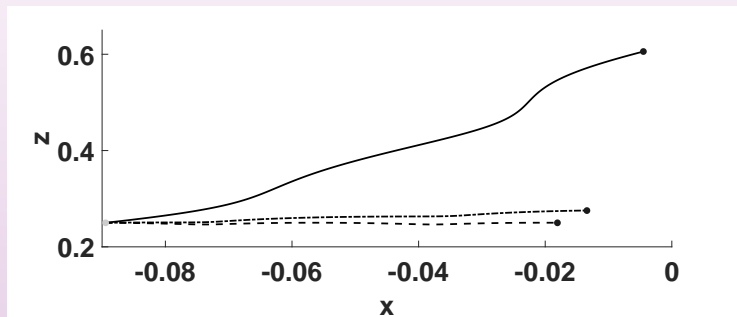


Figure: Paths of the left-side vortex moving under a cnoidal wave for  $0 \leq t \leq 5$  for Froude numbers  $F = 0$  (dashed line),  $.02$  (dashed/dotted line), and  $.2$  (solid line).

# Numerics: Cnoidal Waves

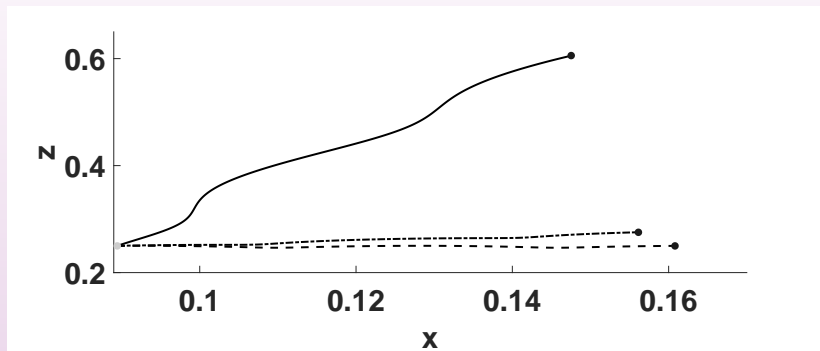


Figure: Paths of the right-side vortex moving under a cnoidal wave for  $0 \leq t \leq 5$  for Froude numbers  $F = 0$  (dashed line),  $.02$  (dashed/dotted line), and  $.2$  (solid line).

# Numerics: Cnoidal Waves

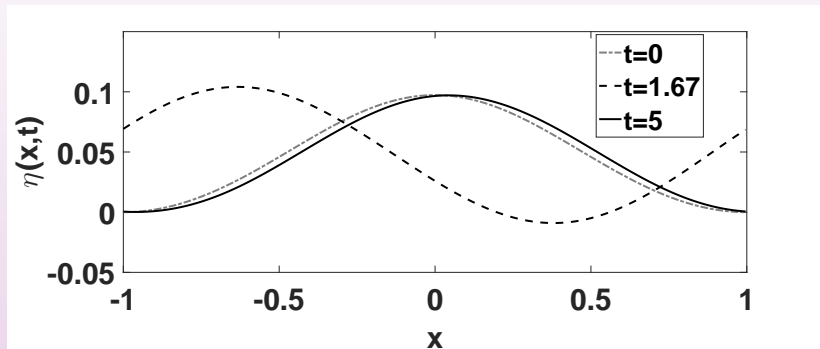


Figure: Surface response  $\eta(x, 5)$  elliptic modulus  $\tilde{m} = .2$  and Froude number  $F = .02$ .

# Numerics: Cnoidal Waves

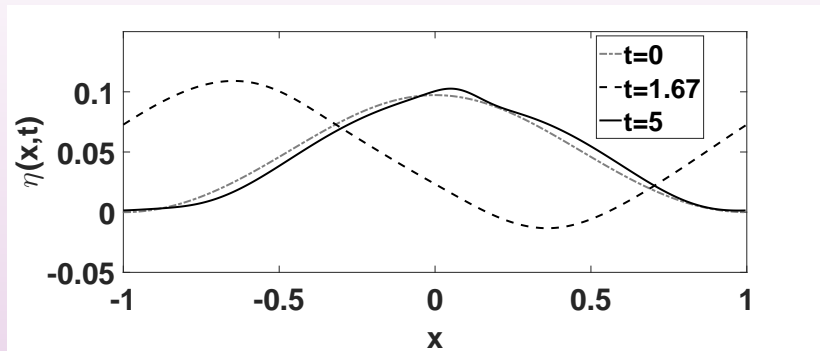


Figure: Surface response  $\eta(x, 5)$  with elliptic modulus  $\tilde{m} = .2$  and Froude number  $F = .2$ .

# Two Counter Propagating Vortices

- Start from a quiescent surface.

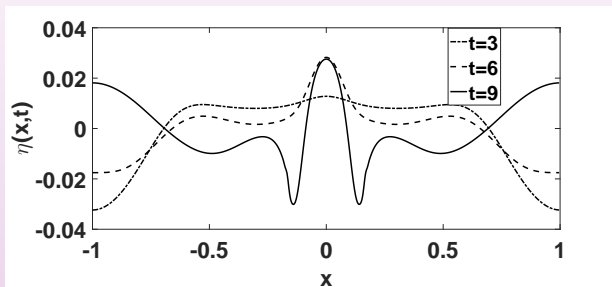
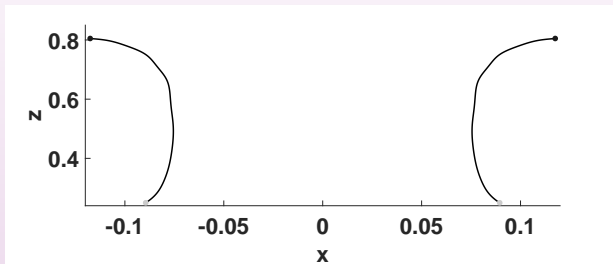


Figure: Surface response  $\eta(x, t)$  at  $t = 3$ ,  $t = 6$ , and  $t = 9$  over two counter-propagating vortices.  $F = .2$

# Two Counter Propagating Vortices



**Figure:** Motion of the two counter-propagating vortices for  $0 \leq t \leq 9$ . The light grey dots indicate where the vortices begin and the black dots indicate their positions at  $t = 9$ .  $F = .2$

# Two Counter Propagating Vortices

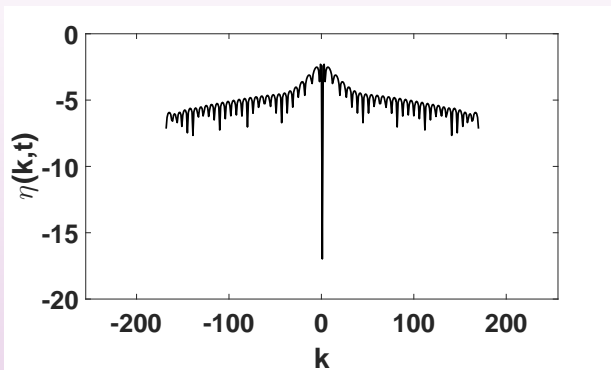


Figure: Log plot of the power spectrum at  $t = 9$  over wave numbers  $-256 \leq k \leq 256$ . As can be seen, the rising vortices pump more energy into higher wavenumbers in the surface profile.

# Two Counter Propagating Vortices

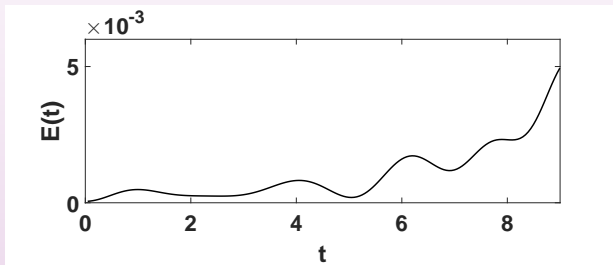


Figure: Surface energy profile  $E(t)$  for a surface over two vortices for  $0 \leq t \leq 9$ .

# Four Counter Propagating Vortices

- Place four vortices at

$$x_1(0) = -2\mu\gamma - \mu\gamma/2, \quad x_2(0) = -2\mu\gamma + \mu\gamma/2,$$

$$x_3(0) = 2\mu\gamma - \mu\gamma/2, \quad x_4(0) = 2\mu\gamma + \mu\gamma/2,$$

$z_j(0) = .25$  in  $+/+$ ,  $-/-$  configuration. Take  $F = .2$ .

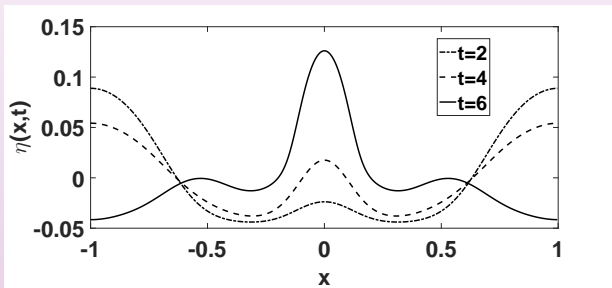


Figure: Surface response  $\eta(x, t)$  for  $t = 2, 4,$  and  $6$  over four vortices in the Plus/Plus, Minus/Minus configuration.

# Four Counter Propagating Vortices

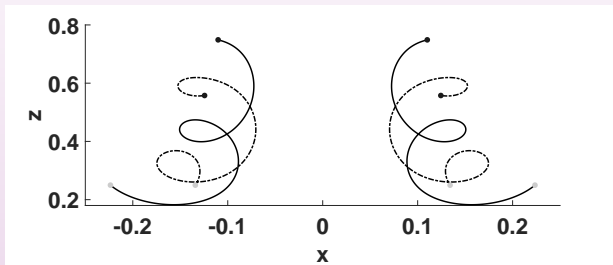


Figure: Motion of four vortices in the Plus/Plus, Minus/Minus configuration for  $0 \leq t \leq 6$ .

# Four Counter Propagating Vortices

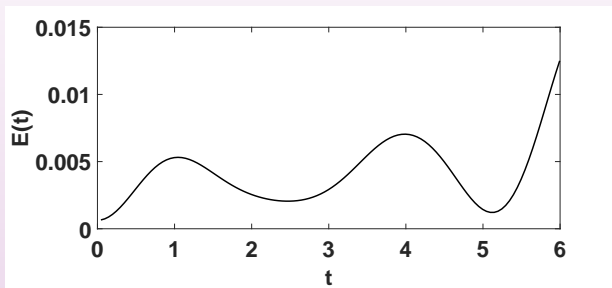


Figure: Surface energy profile  $E(t)$  in response to the motion of four vortices in the Plus/Plus, Minus/Minus configuration for  $0 \leq t \leq 6$ .